Proceedings of the ASME 2021 Conference on Smart Materials,
Adaptive Structures and Intelligent Systems
SMASIS2021
September 14-15, 2021, Virtual, Online

SMASIS2021-68331

FUSED FILAMENT FABRICARION OF CONTINOUS FIBER-REINFORCED THERMOPLASTICS FOR COMPLIANT MECHANISMS

Mohamed Refat
Department of Industrial Engineering, University of Bologna, Italy

Luca Luzi
Department of Computer Science, University of Verona, Italy

Lorenzo Agostini
Department of Industrial Engineering, University of Bologna, Italy

Riccardo Pucci
Department of Industrial Engineering, University of Bologna, Italy

Giovanni Berselli
Department of Mechanical, Energy, Management and Transportation Engineering, University of Genoa, Italy

Rocco Vertechy
Department of Industrial Engineering, University of Bologna, Italy

ABSTRACT

In the last decade composite materials, previously almost exclusively used in aerospace and automotive industries, are becoming widespread thanks to the introduction of the fused filament fabrication (FFF) process in the additive manufacturing technology. With respect to the standard and more widely used material subtractive technologies, the FFF layer-by-layer construction process is capable of manufacturing parts featuring very complex geometry. Moreover, the deposition of reinforcing filaments provides components with high-performance mechanical characteristics.

Since FFF is a relatively new technology, studies are still needed to fully understand the mechanical behavior of composite materials realized with FFF and how all the process parameters (e.g., layer thickness, filament deposition direction, type of matrix and reinforcement, the interaction between matrix and reinforcement) affect the final result.

This paper deals with the preliminary experimental analysis of straight beams realized in carbon-fiber-reinforced Nylon White composite material with the MarkForged MarkTwo three-dimensional printer. Envisaged application of the considered straight beams is as flexible elements in compliant mechanisms. In particular, tensile and bending tests are performed on nine different straight beam specimens in order to provide a first understanding on how the filament disposition within the sample affects its mechanical response.

From the results it is found that the proper position of the reinforcement filaments provides a very effective means to tune the selective compliance of beam flexures.

Keywords: Additive Manufacturing, Composites, Continuous Fiber-Reinforced Thermoplastics, Compliant Mechanisms, Straight Beam Flexures.

1. INTRODUCTION

Compliant mechanisms (CMs) are mechanical systems that transmit motion and forces between rigid elements via the deformation of their flexible members [1,2]. Due to the lack of kinematic pairs, CMs do not suffer from backlash, friction and the need for lubrication. Thus, they reveal to be very suitable for demanding applications that require high-precision, miniaturization and operation in challenging environments (such as hygienic, vacuum, or dirty). Moreover, given the intrinsic energy-storing capabilities of their flexible elements, CMs naturally lend themselves also to the realization of passive force compensators as well as of resonating mechanisms which can be used to reduce the motor requirements of machines operating in both static and cyclic dynamic conditions.

Flexible elements used in CMs can be of different types, from slender beams (usually referred to as beam flexures) featuring distributed compliance to notch hinges with concentrated compliance [1-4]. The specific choice of type,

Copyright © 2021 by ASME

shape and size of the flexible element is typically done based on application requirements [1-4]. Commonly, beam flexures are considered for large ranges of motion and fatigue lifetime, whereas notch hinges are used when resistance to parasitic motions is of paramount importance.

Despite the above-mentioned advantages, the diffusion of CMs is still limited. A major problem is their manufacturing. Traditional subtracting material technologies indeed either lack the required precision or are very expensive for the realization of monolithic structures that include slender (i.e., flexible) and stocky (i.e., rigid) features. In this context, additive manufacturing can be a game-changing technology [5].

Additive manufacturing (also referred to as three-dimensional printing) creates parts by depositing material layer upon layer in precise geometric patterns [5,6]. This approach has considerable advantages, including the realization of complex geometries, regardless of manufacturing skills or labour cost [6]. Several flexible elements, as well as CMs made thereof, have been realized via three-dimensional printing: notch hinges were manufactured via selective laser sintering [7] and material extrusion [8] technologies; a tri-spiral hinge [9] and a prismatic joint [10] were created with fused filament fabrication; a contact-aided compliant mechanism called a twist compliant mechanism has been fabricated using stereolithography [11]; cross-axis flexural pivots and lattice flexures have been made using electron beam melting [12]; a planar compliant force-inverter [13] was realized using multi-material jetting of photopolymers.

Among the additive manufacturing technologies, the Fused Filament Fabrication of Continuous Fiber Reinforced Thermoplastics (FFF-CFRT) combines the possibility of realizing complex shapes and the ease-of-use of plastic-base deposition processes with the ability to obtain material strengths closed to those of metals as well as inhomogeneous and anisotropic material properties. These features can be exploited to realize flexible members, as well as CMs made thereof, with unique properties such as large ranges of motion, selective compliance to minimize parasitic motions, significant mechanical resistance and durability.

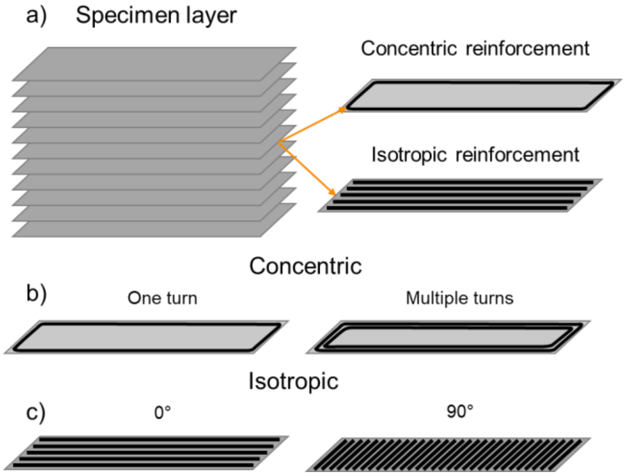

FIGURE 1: DEPOSITION METHODS: a) MIXED, b) CONCENTRIC, c) ISOTROPIC.

Despite the potentialities, research work devoted to the study and application of flexible elements and CMs realized with FFF-CFRT are only a few and very recent; in particular: a compliant lever has been conceived for a locking mechanism in an ankle prosthesis [14]; a camber morphing wing has been developed for drones [15].

In this context, this paper reports on a preliminary investigation on the tensile and flexural response of Straight Beam Flexures (SBF) realized with FFF-CFRT and featuring different interlayer fiber volume-fraction and orientation, as well as different layer stacking sequences.

The paper is organized as follows: Section 2 describes the characteristics and the manufacturing of the SBF considered for the tests, as well as the custom-developed bending and tensile stages used for the experimentation; Section 3 reports and discusses the obtained experimental results.

2. MATERIALS AND METHODS

MarkForged MarkTwo printer is a compact printer with a 320 mm x 231 mm x 154 mm workspace, which can deposit continuous fiber filaments within nylon or Onyx (namely, a thermoset plastic composed of nylon filled with chopped carbon fiber) matrix.

Several reinforcing continuous fibers can be used both with nylon and Onyx: carbon fiber (CF), Kevlar, fiberglass and high-strength high-temperature fiberglass. MarkTwo has two nozzles for material deposition: one is for the matrix material and the other one for the reinforcing continuous fiber.

When CF is chosen, the printing layer thickness of 0.125 mm is set by the slicing software. CF deposition can occur according to two methods (FIGURE1):

1) Circumferential pattern: following the external shape of the component, the CF nozzle covers the printing surface from the outside to the inside, depositing the concentric filament. The filament amount over the surface is a parameter that can be decided by the user. Briefly, if a single filament is selected as reinforcement, it is placed near (the distance is a parameter that can be selected) the outer edge. Additionally, the user can decide which layer is to be provided with reinforcement.
2) Isotropic pattern: the CF deposition on the layer occurs along a certain direction whose orientation is a parameter to be set. In this case, the amount of reinforcement to be used cannot be decided by the user.

The MarkTwo printer has been employed to realize the composite SBF to be experimentally tested. CF reinforced Nylon White (CFRNW) material is used for all the samples with different amounts of reinforcement filaments on the various layers. Fiber arrangement within each specimen has been chosen so as to verify the dependency of tensile and flexural responses of CFRNW SBF on the amount of filament in a layer and on the positioning of the reinforced layers within the beam.

The aspects to be verified with the tests are the following:

Copyright © 2021 by ASME

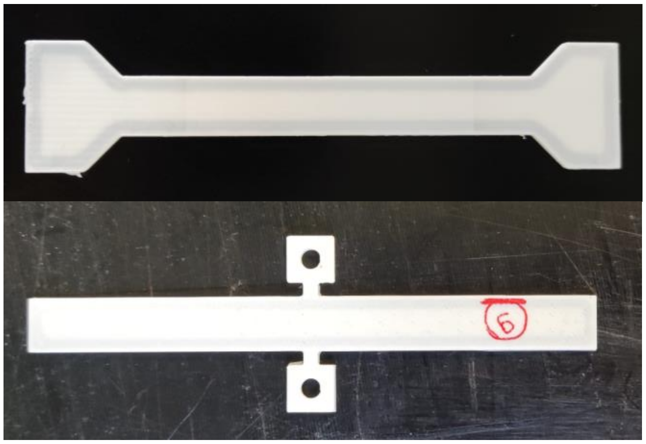

FIGURE 2: TENSION (TOP) AND BENDING (BOTTOM) SAMPLES.

- if longitudinal fibers are placed in the central layer of the sample, the tensile response of the SBF increases with the number of fibers, while leaving almost unchanged the flexural response;
- the different positioning of the same number of longitudinal fibers within the SBF has a minimal influence on the tensile response but a major one on the flexural response, with the flexural stiffness increasing as the fibers are placed farther from the central layer of the sample;
- if the placement of transversal fibers has some effect on the tensile and flexural responses of the SBF.

Every sample (FIGURE 2) is rectangular with an active length of 65 mm for tensile tests and 98 mm for the bending tests, a width of 11.5 mm and a thickness of 1.375 mm (namely 11 layers so that the 6-th layer is the central one). The sample used in the tension test is realized with a particular shape (dog-bone-like) in order to increase the holding surfaces, whereas the bending test sample is provided with a peculiar geometry that enables it to be mounted with precision.

For each campaign, 9 samples with different arrangements of the fibers embedded in the matrix are tested:

1) without reinforcement;
2) one circumferential filament in the 6-th layer;
3) two circumferential filaments in the 6-th layer;
4) three circumferential filaments in the 6-th layer;
5) four circumferential filaments in the 6-th layer;
6) four circumferential filaments in the 6-th layer, plus other filaments in isotropic arrangement with 90° orientation (with respect to the longitudinal direction) in the 3-th and 9-th layers;
7) two circumferential filaments in the 3-th and 9-th layers;
8) two circumferential filaments in the 4-th and 8-th layers;
9) two circumferential filaments in the 5-th and 7-th layers;

Samples 7-9 are provided with the same number of CF fibers as the sample 5.

In the next paragraph, the two test benches used to execute tension and bending experiments are described.

2.1 Tensile test bench

The tensile test bench (FIGURE 3) is composed by a fixed frame (1), a load cell (2) (NS WL 1-500 kg), an electro-cylinder made by a brushless servo motor and a ball-screw transmission (3) (Parker ETH050 M05 High Force Ball-screw Driven Electro Cylinder with the driver Parker SLD2N), and two clamps (4 and 5). Each clamp is tightened on one side to the sample (6) by means of screws and on the other side to the load cell (2) and the electro-cylinder (3), respectively. Furthermore, an extensometer (7) (HBM DD1 ZV11) is mounted on the sample. The electro-cylinder and the load cell are connected to the frame so that the sample longitudinal axis coincides with the axes on which the force is applied and measured. Thanks to the frame high machining accuracy, the alignment of the load cell axis with the applied force axis is guaranteed. The extensometer is provided with sharp knife edges and is kept in contact with the sample through rubber bands. Test-bench control and data acquisition are performed at 1 kHz sampling rate with an industrial PC (Beckhoff CX5120-0125) equipped with strain gauge input modules (Beckhoff EL3356) that are used to acquire both loadcell and extensometer signals.

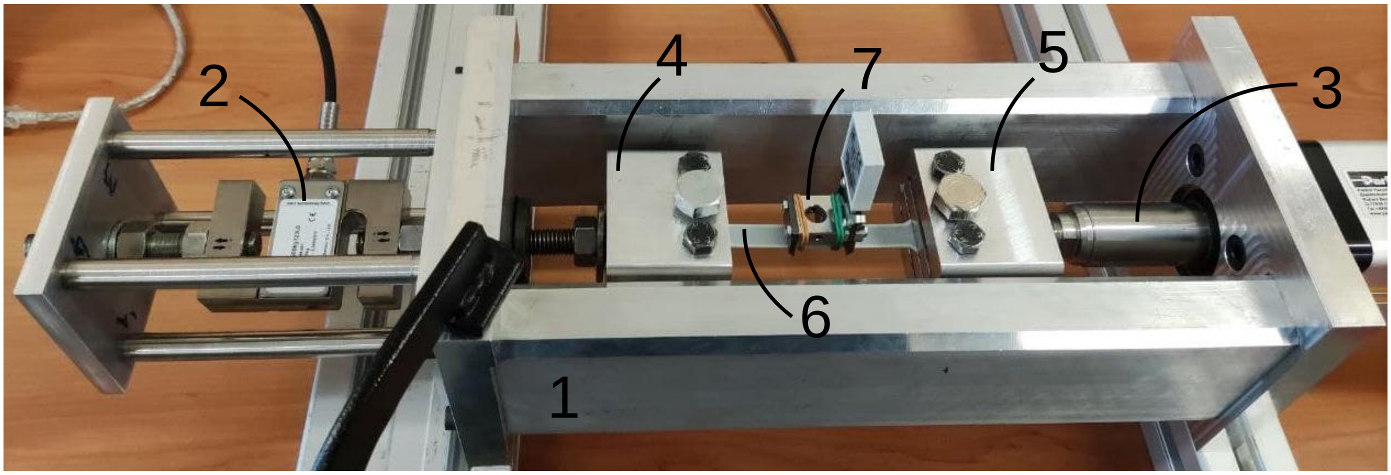

FIGURE 3: TENSION TEST BENCH.

Copyright © 2021 by ASME

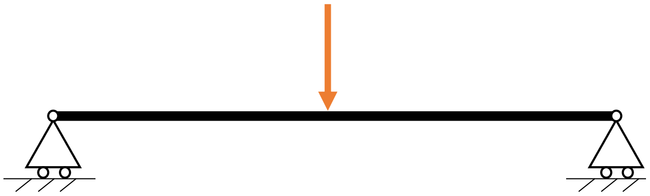

FIGURE 4: BENDING TEST BENCH SCHEMATIC.

The testing procedure is executed according to the following steps:

1) the sample is properly connected to clamps (4) and (5), followed by the mounting of the extensometer;
2) the linear actuator applies a traction force of 6 N to check for misalignments of the components with respect to the force direction. This is considered the sample homing position for the tensile test-bench;
3) a constant velocity of 0.25 mm/s is commanded to the electro-cylinder till a strain of 0.7% is obtained due to the sample stretching. As soon as the strain value is reached, the sample is brought back to its homing position with the same constant velocity in the opposite direction;
4) step 3 is repeated 4 times.

2.2 Bending test bench

As depicted in FIGURE 4, the arrangement used to perform the bending tests consists of a beam (the sample) that is connected at either ends to the frame by means of a revolute and a prismatic pair, and loaded at its middle point. The physical implementation of the test-bench is pictured in FIGURE 5 and is composed by a frame (8) connected to two sliders (9 and 10) (which share the same rail) and an electro-cylinder (11). Two clamps (12 and 13) are tightened to each edge of the sample (14). On the other side, they are connected to (9) and (10) by means of roller bearings. Two encoders (15 and 16) (TRINAMIC motion control TMCS-28) are used to measure the rotation of the clamps with respect to the respective slider. Laser distance sensors (17) and (18) (Panasonic HG-C1050) are used to measure the displacement of the sliders. A load cell (19) (NS-WL1-5 kg) is connected to the electro-cylinder and to a clamp (20) which is tightened to the middle of the sample by means of two screws and a metallic plate placed underneath (see FIGURE 6). Through the electro-cylinder (the same used for the tension test bench) a known displacement is imposed to (20) and the applied force is measured by the load cell. Lasers and encoders measure the displacement and orientation of each edge of the sample. Thanks to the frame high machining accuracy, the slider translation axis is orthogonal to the force axis. To properly position the sample with respect to the force direction, (14) and (20) are provided with reference surfaces (FIGURE 6) that have to be matched during the mounting phase. Monitoring and controlling signals are managed at 1 kHz sampling rate by an industrial PC (Beckhoff CX5120-0125) equipped with data acquisition modules (Beckhoff EL3356, for the loadcell; two Beckhoff EL3702, for laser position sensors; two Beckhoff EL5101, for the rotary encoders; Beckhoff EL1014 for the limit switch of the linear electro-cylinder).

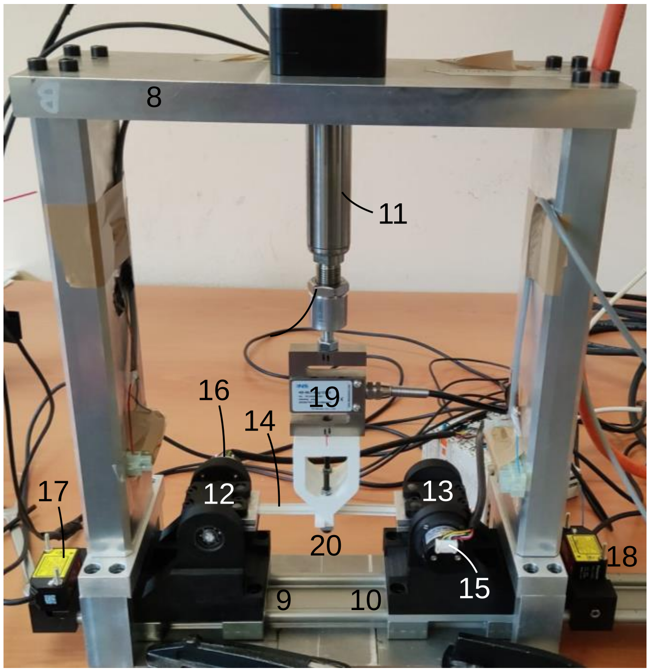

FIGURE 5: BENDING TEST BENCH.

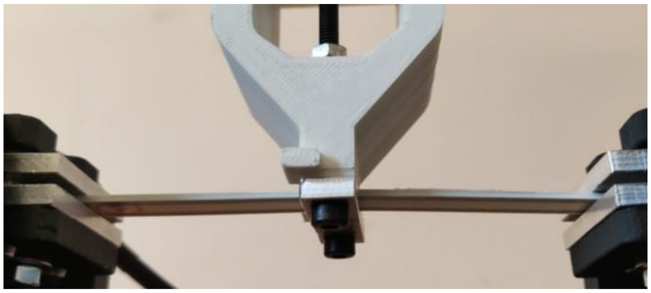

FIGURE 6: CONNECTION BETWEEN THE CLAMP AND THE SAMPLE.

The testing procedure is executed according to the following steps:

1) the sample is properly connected to clamps (12) and (13);
2) the electro-cylinder is moved to the homing position (namely, the position in which the sample is parallel to the rail axis and orthogonal to the electro-cylinder axis) and it is connected with the sample through clamp (20);
3) the encoders (15,16) and the lasers (17,18) are set to the zero rotation and position, respectively;
4) a constant velocity of 2.5 mm/s is commanded to the electro-cylinder till, following the deformation of the sample, the encoders read a rotation of 18°;
5) step 4 is repeated 4 times.

Copyright © 2021 by ASME

3. RESULTS AND DISCUSSION

Results obtained from tensile experimental tests are shown in FIGURE 7 and FIGURE 8, whereas those from the bending tests are shown in FIGURE 9 and FIGURE 10.

The results are grouped in two sets: samples (1-6) with CF deposited along the longitudinal direction only in the central layer (central plane) and samples (7-9) with CF deposited along the longitudinal direction far from the central plane (in FIGURE 8 and FIGURE 10, both samples (5) and (6) are shown to compare the two sets).

From the tensile stress-strain curves of the first set (FIGURE 7), the stress value at 0.7% strain markedly increases with the number of CF filaments deposited. The maximum value of 40MPa is reached by the sample (6), meaning that isotropic fibers at 90° also contribute to increasing the tensile stiffness. The minimum value of 9 MPa is reached by sample (1), with no fibers, as expected.

Regarding the bending test results (FIGURE 9), samples (1-5) show a similar trend, proving that the fiber filaments deposited on the central layer do not significantly affect the flexural stiffness. Also in this case, the highest value of the bending moment (35 Nmm) is reached by the sample (6), meaning that isotropic fibers at 90° also contribute to increasing the flexural stiffness. The mean value of the maximum moment computed for samples (1-5) is 14.8 Nmm with a standard deviation of 1.4 Nmm. The lowest value is achieved by sample (1).

With reference to the set of tensile tests reported in FIGURE 8, samples (5-9) exhibit a similar behavior. The mean value of the maximum tensile stress is 39.1 MPa with a standard deviation of 3.67 MPa.

FIGURE 10 shows the effect of the deposition of the fibers far from the central layer. The highest maximum moment value (51 Nmm) is reached by sample (7) with fibers on the more external layers, whereas the lowest value (17 Nmm) of the maximum moment is achieved by sample (5) with fibers in the central layer. Comparison of samples (7) and (6) clearly highlights the minor effect on the bending stiffness of adding transversal fibers rather than of longitudinal fibers in the outer layers (the maximum bending moment for sample (6) is 35 Nmm, that is just 68% of the one measured for sample (7)).

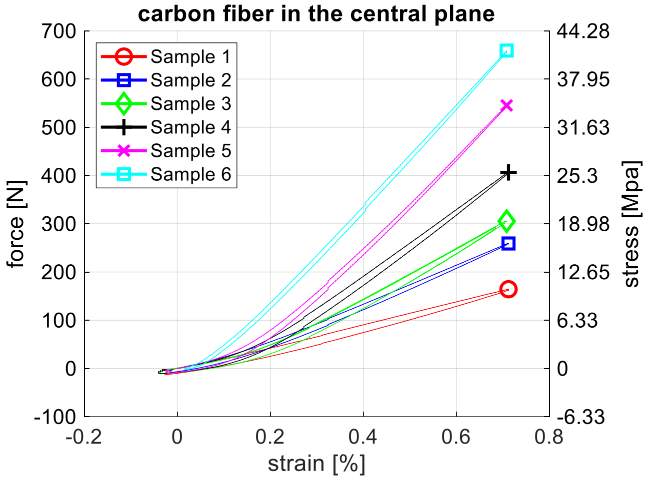

FIGURE 7: TENSILE TEST RESULT FOR SAMPLES 1-6

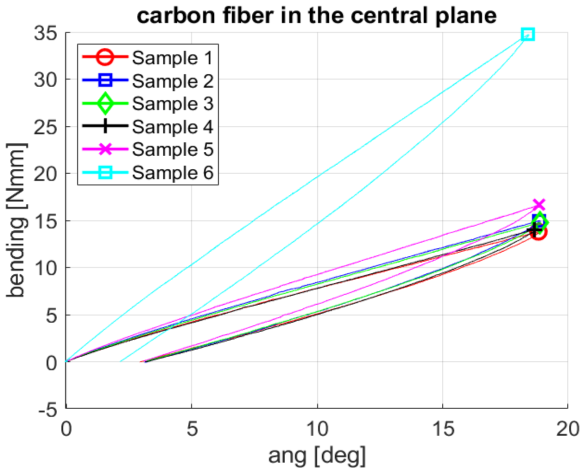

FIGURE 9: BENDING TEST RESULT FOR SAMPLES 1-6

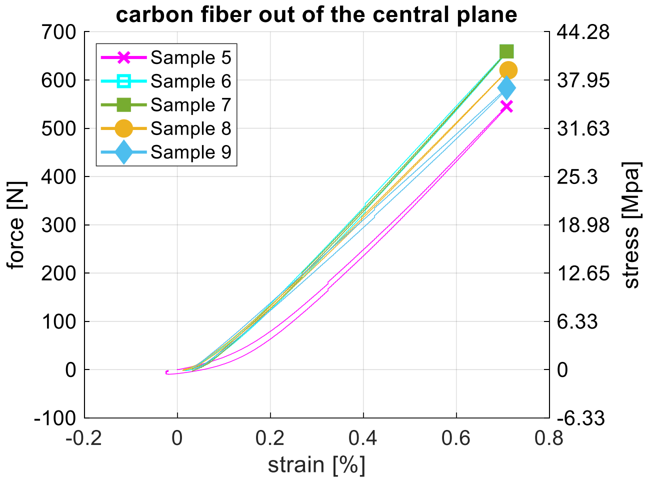

FIGURE 8: TENSILE TEST RESULT FOR SAMPLES 5-9

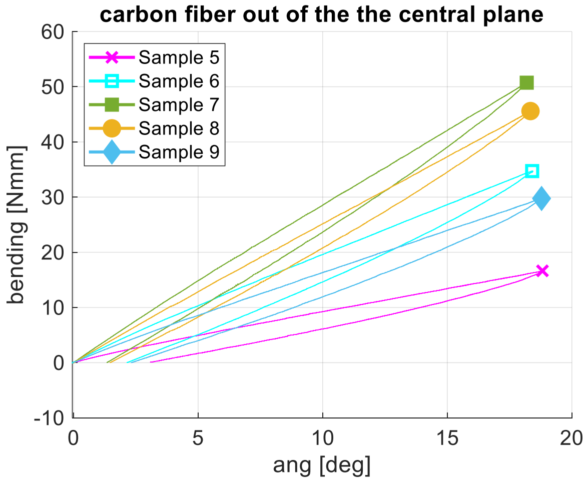

FIGURE 10: BENDING TEST RESULT FOR SAMPLES 5-9

Copyright © 2021 by ASME

4. CONCLUSION

This paper deals with the experimental analysis of straight beam flexures (SBF) realized in carbon fiber reinforced Nylon White material with the fused filament fabrication machine MarkTwo commercialized by MarkForged. Tests are executed in order to assess the dependency of the tensile and flexural responses of the considered SBF on the arrangement of the continuous carbon fibers within the polymeric matrix. In particular, the effect of the filament position with respect to the central layer is studied. Nine samples are considered: the first is printed without reinforcement; samples from 2-th to 6-th have reinforcement on the central layer along the longitudinal direction (the 6-th sample is also provided with filaments with a direction orthogonal to the longitudinal axis in the external layers); the last three samples are printed with reinforcing filaments placed symmetrically with respect to the central layer.

The experimental results revealed the following:

1) When a stretching force is applied, the disposition of the longitudinal fibers (circumferential pattern) within the sample does not affect the tensile stiffness. This latter is dependent only on the number of fibers (e.g., samples (5), (7), (8) and (9) having the same number of longitudinal fibers exhibit the same tensile stiffness).
2) When a bending moment is applied, the amount of longitudinal fibers deposited on the central layer does not have an effect on the flexural stiffness (i.e., samples (2-5) with a different number of fibers in the central layer show a similar flexural response, which is almost the same to that of the unreinforced sample (1)). On the contrary, the circumferential deposition out of the central layer plays a key role (e.g., sample (7)).
3) The deposition of transversal fibers (sample (6)) lightly increases both the tensile and flexural stiffness. In order to properly characterize the contribution of the transversal fibers, other experimental tests need to be conducted.

Overall, the reported results show that for the same geometry and amount of material, SBF mechanical characteristics can be tuned by simply changing the disposition of the fibers within the matrix. This feature perfectly fits the needs of compliant mechanisms, which require flexible elements with selective compliance that has to be selectable based on the application.

ACKNOWLEDGMENTS

The Italian Ministry of Foreign Affairs and International Cooperation (MAECI) is deeply acknowledged for funding this work.

The authors would also like to thank Mr. Amedeo Carloni and Mr. Marco Caselli for their assistance in conducting the experimental tests and their support in revising the manuscript.

REFERENCES

[1] L. L. Howell, S. P. Magleby, and B. M. Olsen, Handbook of Compliant Mechanisms. 2013.

[2] N. Lobontiu and E. Garcia, “Analytical model of displacement amplification and stiffness optimization for a class of flexure-based compliant mechanisms,” Comput. Struct., vol. 81, no. 32, 2003, doi: 10.1016/j.compstruc.2003.07.003.

[3] B. P. Trease, Y. M. Moon, and S. Kota, “Design of large-displacement compliant joints,” J. Mech. Des. Trans. ASME, vol. 127, no. 4, 2005, doi: 10.1115/1.1900149.

[4] D. F. Machekposhti, N. Tolou, and J. L. Herder, “A review on compliant joints and rigid-body constant velocity universal joints toward the design of compliant homokinetic couplings,” Journal of Mechanical Design, Transactions of the ASME, vol. 137, no. 3. 2015, doi: 10.1115/1.4029318.

[5] J. S. Cuellar, G. Smit, D. Plettenburg, and A. Zadpoor, “Additive manufacturing of non-assembly mechanisms,” Additive Manufacturing, vol. 21. 2018, doi: 10.1016/j.addma.2018.02.004.

[6] I. Gibson, D. Rosen, B. Stucker, and M. Khorasani, Additive Manufacturing Technologies. 2021.

[7] M. W. M. Groenewegen, M. E. Aguirre, and J. L. Herder, “Design Of a partially compliant, three-phalanx underactuated prosthetic finger,” in Proceedings of the ASME Design Engineering Technical Conference, 2015, vol. 5A-2015, doi: 10.1115/DETC2015-47055.

[8] R. Mutlu, G. Alici, M. In Het Panhuis, and G. Spinks, “Effect of flexure hinge type on a 3D printed fully compliant prosthetic finger,” in IEEE/ASME International Conference on Advanced Intelligent Mechatronics, AIM, 2015, vol. 2015-August, doi: 10.1109/AIM.2015.7222634.

[9] A. T. Gaynor, N. A. Meisel, C. B. Williams, and J. K. Guest, “Multiple-Material Topology Optimization of Compliant Mechanisms Created Via PolyJet Three-Dimensional Printing,” J. Manuf. Sci. Eng. Trans. ASME, vol. 136, no. 6, 2014, doi: 10.1115/1.4028439.

[10] S. B. Ge, X. C. Duan, P. Li, and T. Zheng, “A compliant translational joint based force/displacement integrated sensor,” in IET Conference Publications, 2015, vol. 2015, no. CP676, doi: 10.1049/cp.2015.1556.

[11] J. A. Mirth, “Preliminary investigations into the design and manufacturing of Fully Compliant Layered Mechanisms (FCLMs),” in Proceedings of the ASME Design Engineering Technical Conference, 2013, vol. 6 A, doi: 10.1115/DETC2013-12124.

[12] Y. Tummala, M. I. Frecker, A. A. Wissa, and J. E. Hubbard, “Design optimization of a twist compliant mechanism with nonlinear stiffness,” Smart Mater. Struct., vol. 23, no. 10, 2014, doi: 10.1088/0964-1726/23/10/104010.

[13] E. G. Merriam and L. L. Howell, “Lattice flexures: Geometries for stiffness reduction of blade flexures,” Precis. Eng., vol. 45, 2016, doi: 10.1016/j.precisioneng.2016.02.007.

[14] F. Heremans, B. Dehez, and R. Ronsse, “Design and Validation of a Lightweight Adaptive and Compliant Locking Mechanism for an Ankle Prosthesis,” in Proceedings of the IEEE RAS and EMBS International Conference on Biomedical Robotics and Biomechatronics, 2018, vol. 2018-August, doi: 10.1109/BIOROB.2018.8487209.

Copyright © 2021 by ASME

[15] U. Fasel, D. Keidel, L. Baumann, G. Cavolina, M. Eichenhofer, and P. Ermanni, “Composite additive manufacturing of morphing aerospace structures,” Manuf. Lett., vol. 23, 2020, doi: 10.1016/j.mfglet.2019.12.004

Copyright © 2021 by ASME